Acetylation modulates prolactin receptor dimerization

Li Ma[a,1], Jin-song Gao[a,1], Yingjie Guan[a], Xiaoyan Shi[a], Hao Zhang[a], Marina K. Ayrapetov[a], Zhe Zhang[a,b], Li Xu[c], Young-Min Hyun[d], Minsoo Kim[d], Shougang Zhuang[e], and Y. Eugene Chin[a,2]

Departments of [a]Surgery and [e]Medicine, Brown University School of Medicine–Rhode Island Hospital, Providence, RI 02903; [b]Department of Surgery, Zhejiang University School of Medicine, Hangzhou, Zhejiang 310058, China; [c]Department of Genetics, Zhejiang Chinese Medical University, Hangzhou, Zhejiang 310058, China; and [d]Department of Immunology, Rochester University, Rochester, NY 14642

Edited by George D. Yancopoulos, Regeneronaceuticals, Inc., Tarrytown, NY, and approved September 24, 2010 (received for review July 21, 2010)

Cytokine-activated receptors undergo extracellular domain dimerization, which is necessary to activate intracellular signaling pathways. Here, we report that in prolactin (PRL)-treated cells, PRL receptor (PRLR) undergoes cytoplasmic loop dimerization that is acetylation-dependent. PRLR-recruited CREB-binding protein (CBP) acetylates multiple lysine sites randomly distributed along the cytoplasmic loop of PRLR. Two PRLR monomers appear to interact with each other at multiple parts from the membrane-proximal region to the membrane-distal region, relying on the coordination among multiple lysine sites neutralized via acetylation. Cytoplasmic loop-dimerized PRLR activates STAT5, which is also acetylated by CBP and undergoes acetylation-dependent dimerization. PRLR dimerization and subsequent signaling are enhanced by treating the cells with deacetylase sirtuin (SIRT) inhibitor nicotinamide or histone deacetylase (HDAC) inhibitor trichostatin A but inhibited by expressing exogenous deacetylase SIRT2 or HDAC6. Our results suggest that acetylation and deacetylation provide the rheostat-like regulation for the cytokine receptor PRLR in its cytoplasmic loop dimerization and subsequent STAT5 activation.

acetylation | CREB-binding protein | dimerization | prolactin receptor | STAT5

Type I cytokine receptors share a common structure of an extracellular ligand-binding domain bearing a conserved "WSXWS" motif, a single transmembrane helix, and a cytoplasmic loop (Table S1). Prolactin receptor (PRLR) is an essential type I cytokine receptor involved in mammary gland development during pregnancy and lactation. On ligand binding, the membrane-proximal regions of the PRLR cytoplasmic loop are brought into defined proximity to ensure activation of the protein kinase JAK2, which docks within the membrane-proximal proline box (1, 2). JAK2 phosphorylates PRLR on multiple tyrosine sites along the loop and the loop-associated STAT5a, and STAT5b on a conserved tyrosine residue within the C-terminal SH2-dimerization domain. Subsequently, tyrosine-phosphorylated STAT5 dissociates from the receptor, forms a transcriptional active dimer, and translocates into the nucleus, where it regulates gene expression associated with the functions of the ligand prolactin (PRL). Associated with one monomer of a dimer, JAK phosphorylates STAT docked along the loop of the other receptor molecule of the dimer, requiring a close proximity between two receptor molecules in their cytoplasmic loops (3–5). The cytoplasmic loops of type I cytokine receptors can be very different in size, ranging from 31 to 568 residues, with no apparent homology in primary sequences (Table S1). Both the number and location of positively charged lysine may affect two cytoplasmic loops to reach close proximity during homodimerization.

Here, we show that PRL-activated PRLR and its downstream STAT5b were both highly acetylated by CREB-binding protein (CBP). By recruiting CBP, the PRLR cytoplasmic loop was acetylated on multiple lysine sites along the loop that work together to neutralize the positive charge of lysine side chain, weaken the electrostatic resistance, and allow two receptor molecules to reach a close proximity for homodimerization within their cytoplasmic loops. PRLR-recruited STAT5b, conversely, was activated largely via K694 acetylation-dependent dimerization. Acetylation-dependent cytoplasmic loop dimerization has been shared as a mechanism for activation among type I cytokine receptors that activate STAT.

Results

PRLR Is Acetylated by CBP on Multiple Sites Along Its Cytoplasmic Loop. In human breast cancer T47D cells, PRL treatment induced PRLR acetylation, which was moderately but repeatedly enhanced by pretreatment of the cells with the deacetylase sirtuin (SIRT) inhibitor nicotinamide (NAM) (Fig. 1*A* and Fig. S1*A*). PRL-induced PRLR acetylation in T47D cells was largely abolished when CBP was depleted by transient transfection with specific siRNA (Fig. 1*B*). CBP-mediated acetylation of PRLR was reversed if the deacetylase SIRT2 or, to a lesser extent, SIRT1 or histone deacetylase (HDAC) family member HDAC6 or HDAC3 was overexpressed (Fig. 1*C* and Fig. S1*B*). Treating the transfectants with NAM or the HDAC inhibitor trichostatin A (TSA) could moderately but repeatedly elevate PRLR acetylation (Fig. 1*C*). Among the histone acetyltransferases (HATs) tested in a transient transfection analysis, CBP or, to a much lesser extent, p300 overexpression catalyzed PRLR acetylation in human embryonic kidney 293T cells (Fig. S1*C*). To narrow down the acetylation regions, we generated a series of Myc-tagged PRLR cytoplasmic loop truncates that lack the extracellular and transmembrane domains (Fig. S1*D*) and examined their acetylation by CBP cotransfection in 293T cells. The acetylation intensity reduced proportionally when the cytoplasmic loop was proportionally truncated (Fig. 1*D*). CBP appeared to acetylate the PRLR cytoplasmic loop in multiple regions from the C terminus to the membrane-proximal region. Hence, PRLR can be acetylated by CBP, a process that can be reversed by both SIRT type and HDAC type deacetylases in cells.

To map acetylated lysine sites, CBP-acetylated PRLR was immunopurified from 293T transfectants and submitted to MS analysis. Fifteen lysine residues (i.e., K277, K339, K412, K456, K466, K472, K505, K514, K517, K526, K533, K536, K567, K590, and K601) were identified as acetylation sites (Fig. S1*F* and Table S2). These acetyl-lysine sites exclusively but randomly distribute within the cytoplasmic loop of PRLR from the 259–622 region. To examine endogenous PRLR acetylation in response to PRL treatment, we generated rabbit polyclonal antibodies to three randomly selected acetylation sites (i.e., K277, K505, and K526) of PRLR (Fig. S1*E*). In T47D cells, PRLR acetylation on these three sites within 5 min of PRL treatment was clearly detected with these specific antibodies on protein immunoblotting (Fig. 1*E*). A direct effect of CBP on PRLR acetylation was further confirmed by performing an in vitro PRLR acetylation assay in which immunopurified PRLR was incubated with bacterially purified GST-CBP in acetylation reaction buffer, followed by Western blotting with a specific antibody recognizing acetyl-K277 of PRLR (Fig. 1*F*).

Author contributions: L.M., J.-s.G., and Y.E.C. designed research; L.M., J.-s.G., Y.G., X.S., H.Z., M.K.A., Z.Z., L.X., and S.Z. performed research; L.M., J.-s.G., Y.-M.H., M.K., and Y.E.C analyzed data; and L.M. and Y.E.C. wrote the paper.

The authors declare no conflict of interest.

This article is a PNAS Direct Submission.

[1]L.M. and J.-s.G. contributed equally to this work.

[2]To whom correspondence should be addressed. E-mail: y_eugene_chin@brown.edu.

This article contains supporting information online at www.pnas.org/lookup/suppl/doi:10.1073/pnas.1010253107/-/DCSupplemental.

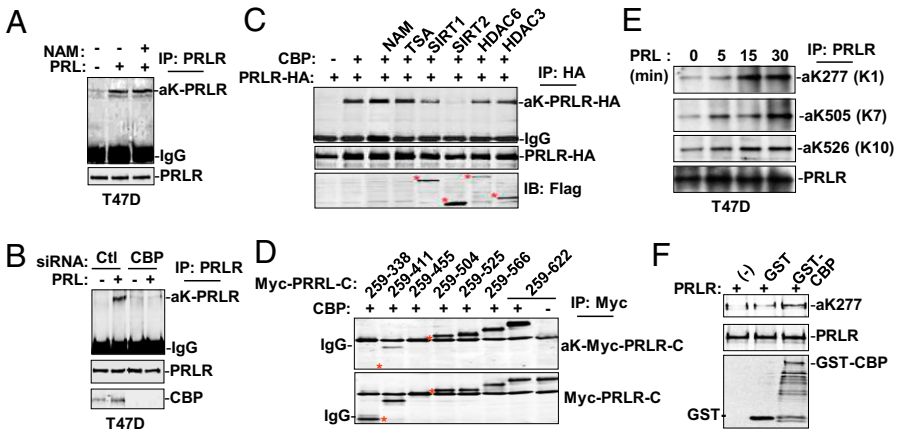

Fig. 1. PRLR cytoplasmic loop is acetylated by CBP. (*A*) T47D cells received no treatment, PRL treatment for 30 min, or NAM (5 mM) pretreatment for 5.5 h, followed by PRL treatment for 30 min. Immunoprecipitated (IP) PRLR was analyzed for acetylated-PRLR (aK-PRLR) with polyclonal antibody to acetyl-lysine. (*B*) In T47D cells, CBP-specific siRNA or control (Ctl) siRNA was transiently transfected, followed by PRL treatment for 30 min. PRLR acetylation was analyzed as above. (*C*) PRLR was cotransfected with CBP in 293T cells, followed by no treatment or treatment with NAM or TSA (1 μM). To test PRLR deacetylation, PRLR and CBP were transfected along with Flag-tagged SIRT1, SIRT2, HDAC6, or HDAC3 in 293T cells, followed by acetylation blotting analysis. (*D*) Myc-PRLR cytoplasmic loop truncation variants (from K259 to a different C-terminal end as illustrated in Fig. S1*D*) were transfected along with CBP in 293T cells, followed by monoclonal anti-acetyl-lysine blotting. (*E*) Endogenous PRLR was immunoprecipitated from T47D cells treated with PRL for different times for acetylation analysis, with specific antibodies recognizing indicated acetylation sites of PRLR. (*F*) GST-CBP-HAT (amino acids 1,196–1,718)–catalyzed PRLR-CD acetylation in vitro was detected with anti-acetyl-K277-PRLR.

CBP Exports from Nuclei to Associate with PRLR in Cytoplasm. CBP is a transcription cofactor localized mainly in the nuclei of quiescent cells, but it undergoes cytoplasmic accumulation in the cells treated with type I IFN (IFN-α) or with UV light (6, 7). In T47D cells, CBP was recovered from anti-PRLR immunoprecipitates in a ligand stimulation-dependent manner (Fig. 2*A*). In T47D cells or another human breast cancer line (MCF-7) cells, a basal level of CBP in cytoplasm was detected (Fig. 2*B*). CBP started to increase its level in cytoplasm by receiving PRL treatment for 5 min (Fig. 2 *B* and *C*), which was independent of JAK tyrosine kinase activity because

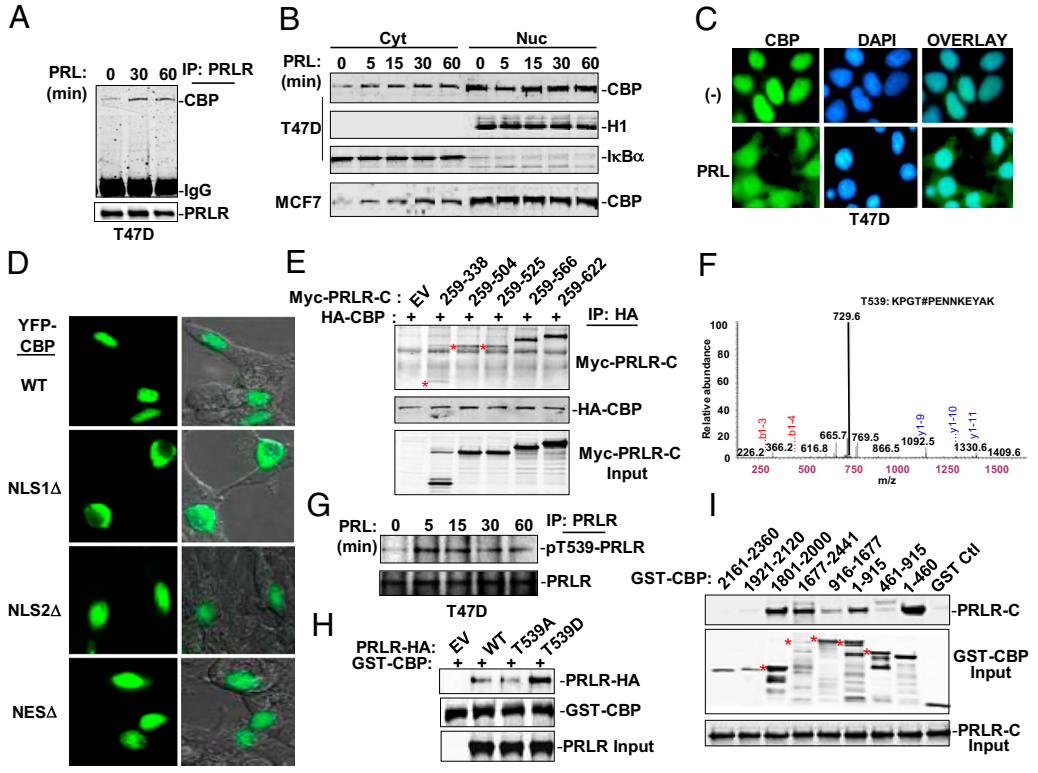

Fig. 2. CBP nuclear exportation on PRL stimulation. (*A*) In T47D cells treated with PRL for different times (as indicated), CBP was recovered from PRLR immunoprecipitate (IP) for Western blot analysis. (*B*) Cytosolic (Cyt) and nuclear (Nuc) fractions were prepared from T47D cells treated with PRL for different times, as indicated, and analyzed for the localization of CBP, histone H1, and IκBα. Dynamic CBP subcellular localization was also analyzed with the cytosolic and nuclear fractions prepared from MCF7 cells receiving PRL treatment. (*C*) CBP was immunostained with monoclonal anti-CBP in T47D cells treated with or without PRL for 60 min. (*D*) YFP-tagged CBP of WT, NLS1 deletion (NLS1Δ), NSL2 deletion (NLS2Δ), or nuclear export signal deletion (NESΔ) form was transiently expressed in 293T cells and visualized with a confocal microscope. (*E*) Empty vector (EV) and Myc-tagged PRLR cytoplasmic loop truncation mutants were cotransfected with HA-CBP and coimmunoprecipitated with HA polyclonal antibody. (*F*) Mass spectrum of the peptide-bearing phospho-T539 of PRLR. (*G*) Immunoprecipitated PRLR from T47D cells treated with PRL for different times, as indicated, was analyzed by Western blotting with anti-pT539-PRLR. (*H*) Purified GST-CBP protein was incubated with whole-cell extracts prepared from 293T cells transfected with empty vector (EV) or PRLR-HA (WT, T539A, and T539D). PRLR proteins were recovered from GST-CBP precipitates in Western blots. (*I*) Indicated GST-CBP domain proteins were purified from bacteria and incubated with Myc-tagged PRLR cytoplasmic domain prepared from 293T transfectants. The CBP-precipitated PRLR cytoplasmic domain was detected by blotting with anti-Myc.

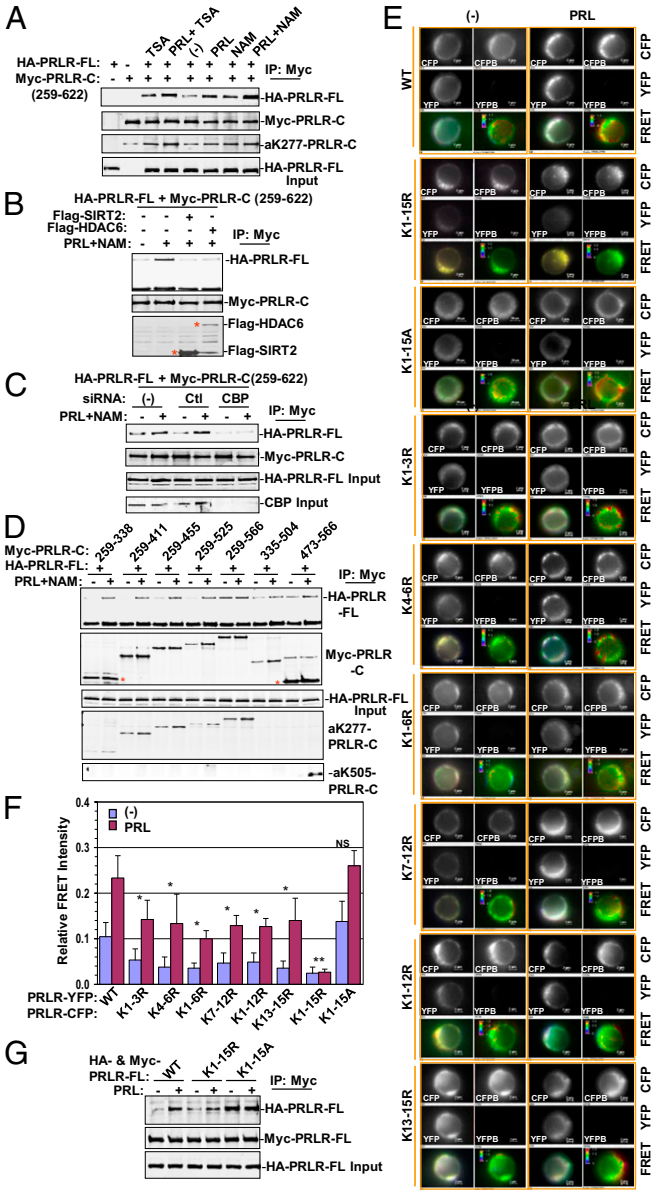

Fig. 3. Acetylation modulates PRLR cytoplasmic loop dimerization. (*A*) HA-PRLR-Full-Length (FL) and Myc-PRLR-Cytoplasmic Domain (C) were cotransfected in 293T cells, followed by no treatment or treatment with PRL, TSA, NAM, PRL plus NAM, or PRL plus TSA for 30 min. Anti-Myc immunoprecipitates (IP) were analyzed with anti-HA, anti-Myc, or anti-aK277-PRLR. (*B*) In 293T cells, HA-PRLR-FL and Myc-PRLR-C were cotransfected with empty vector, Flag-SIRT2, or Flag-HDAC6, followed by no treatment or PRL treatment for 30 min. The Myc immunoprecipitates were analyzed with anti-HA in Western blots (*C*) CBP depletion with siRNA on PRLR-FL and PRLR-C dimerization was analyzed with coimmunoprecipitation. (*D*) In 293T cells, HA-PRLR-FL was cotransfected with Myc-PRLR-C truncates, followed by NAM and PRL cotreatment. Anti-Myc immunoprecipitates were analyzed with anti-HA, anti-aK277-PRLR, or anti-aK505-PRLR. (*E*) FRET images of the indicated pairs of CFP-PRLR and YFP-PRLR expressed in CHO cells, followed by PRL treatment or no treatment. Images of CFP and YFP fluorescence for individual CHO cells before and after YFP bleaching are shown in the upper two rows. The disappearance of YFP fluorescence after bleaching and the increase in CFP fluorescence for WT and K1–15A mutant but not for K1–15R mutant after PRL treatment were observed. (*Left*) Merging of YFP before and after bleach and CFP before and after bleach are shown in the third row. (*Right*) Ratios of CFPpost/CFPpre are shown in the third row. (*F*) FRET efficiency (*y* axis) from the indicated CFP/YFP-tagged constructs in CHO cells treated with or without PRL. For pre- and postphotobleaching image sets of CFP, the cell of interest was selected and the background values were subtracted from the donor pre- and postbleaching. The spectrally corrected FRET efficiency (E) was calculated using the equation E = 1 − (FCFP(d)Pre/FCFP(d)Post) (23), where FCFP(d)Pre and FCFP(d)Post are the mean CFP emission intensity of pre- and postphotobleaching. Data represent the mean ± SEM for three to six cells. When compared with WT, (–), or PRL, $*P < 0.05$ for K1–3R, K4–6R, K1–6R, K7–12R, K1–12R, and K13–15R; $**P < 0.01$ for K1–15R; NS (not significant) for K1–15A. (*G*) HA-tagged and Myc-tagged PRLR-FL of WT, K1–15R, or K1–15A was cotransfected in pairs in 293T cells, followed by PRL treatment for 30 min. Anti-Myc immunoprecipitates were analyzed with anti-HA for PRLR dimerization.

JAK2 depletion in T47D cells did not affect CBP nuclear exportation in response to PRL treatment (Fig. S2*A*). CBP bears two putative nuclear localization signal (NLS) sequences and one putative nuclear export signal (L40PDELIPNGELSL) (Fig. S2*B*). Deletion mutation analysis revealed that NLS1 (P10NPKRAKLS) but not NLS2 (N1591KKTNKNKS-SISRANKKKP) was necessary for nuclear localization of fluorescent-tagged CBP (Fig. 2*D*). NSL1-deleted CBP basically maintained its catalytic activity in PRLR acetylation (Fig. S2*C*).

Overexpression of the above Myc-tagged cytoplasmic loop variants of PRLR along with HA-tagged CBP revealed that the interaction between CBP and the PRLR cytoplasmic loop was attenuated when the cytoplasmic domain truncation was extended from the 525–566 region (Fig. 2*E*), indicating that the 525–566 region is relevant to CBP association. MS analysis revealed that T539 of the proline box (PELPPTPP) within residues 525–566 of PRLR was phosphorylated (Fig. 2*F*). With the rabbit polyclonal antibody generated against T539-phosphorylated PRLR, we detected PRLR phosphorylation on T539, which was inducible by PRL treatment in T47D cells using a polyclonal antibody raised to recognize T539 phosphorylated PRLR (Fig. 2*G* and Fig. S1*E*). We then estimated whether T539 phosphorylation is involved in CBP docking, because CBP can dock on the phosphoserines residing within a proline-rich motif of IFN-αR2 (7). PRLR with T539A but not T539D substitution reduced the association ability of CBP as analyzed with both in vitro and in vivo assays (Fig. 2*H* and Fig. S2*D*), suggesting that phospho-T539 may indeed provide CBP as a docking site. To uncover the domain of CBP responsible for PRLR interaction, GST-fusion proteins of CBP domains (Fig. S2*B*) purified from bacteria were incubated with the cytoplasmic loop of PRLR expressed in 293T cells. The PRLR cytoplasmic loop appeared to associate with CBP within both the N-terminal CH1 domain (amino acids 1–460) and the C-terminal CH3 domain (amino acids 1,801–2,000) (Fig. 2*I*). Given that NSL1 falls within the PRLR-binding domain, NSL1 deletion might partially affect its catalytic activity in PRLR acetylation induction (Fig. S2*C*) by affecting the interaction between these two proteins.

PRLR Cytoplasmic Loop Acetylation on Multiple Sites Coordinates Cytoplasmic Loop Dimerization. Cytokine receptors undergo dimerization induced by the interaction of their extracellular domains. In T47D cell extracts treated with disuccinimidyl suberate, endogenous PRLR proteins were cross-linked into species migrating in SDS/PAGE at the expected position for a dimer (Fig. S3*A*). Under both conditions, PRL treatment enhanced PRLR dimerization, although a basal level of PRLR dimerization was visualized (Fig. S3*A*). The interaction between the cytoplasmic loop and full-length PRLR was induced by treating the cells with PRL, TSA, or NAM either alone or combined (Fig. 3*A*). Both TSA and NAM induced PRLR cytoplasmic loop acetylation in 293T cells as detected with the specific antibody recognizing K277-acetylated PRLR (Fig. 3*A* and Fig. S3*B*). In contrast, the interaction between the PRLR cytoplasmic loop and full-length PRLR was inhibited by transient overexpression of the deacetylase SIRT2 or HDAC6 (Fig. 3*B*) or by depleting CBP with siRNA (Fig. 3*C*). Hence, PRLR cytoplasmic loop dimerization appears to be influenced by reversible acetylation.

To uncover the regions and identify the lysine site(s) responsible for PRLR cytoplasmic loop dimerization, we transfected HA-

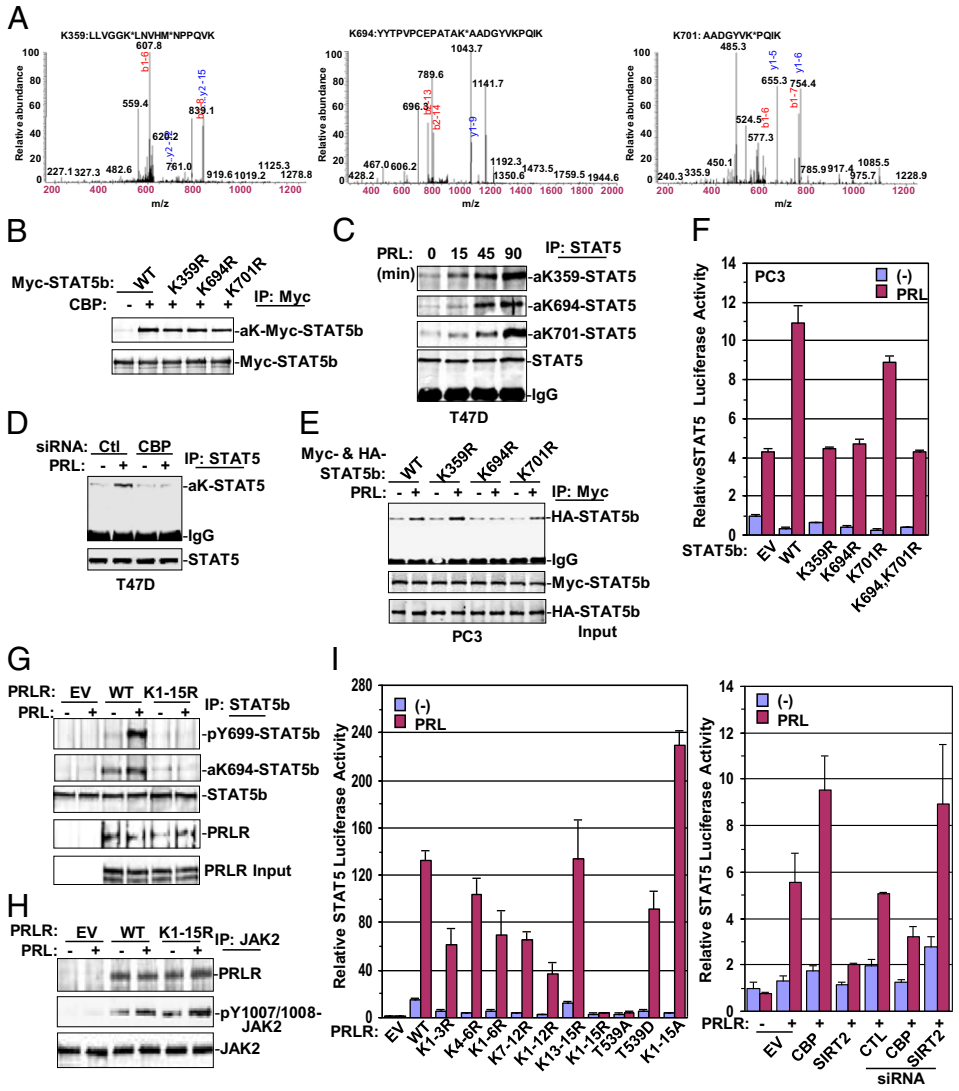

Fig. 4. STAT5 dimerization requires acetylation. (*A*) Mass spectra of acetylated peptides recovered from STAT5b prepared from 293T cells transfected with STAT5 and CBP. (*B*) STAT5b WT and STAT5b with a K→R mutation were transiently transfected along with CBP in 293T cells. Immunoprecipitated (IP) STAT5b proteins were analyzed with pan–anti-acetyl-lysine. (*C*) STAT5 acetylation in T47D cells received PRL treatment for different times and was analyzed with specific polyclonal antibodies against ak359-STAT5b, aK694-STAT5b, and aK701-STAT5b, respectively. (*D*) In T47D, CBP down-regulation with siRNA on STAT5 acetylation (pan–anti-acetyl-lysine) in response to PRL treatment for 30 min. (*E*) In PC3 cells, Myc-tagged and HA-tagged STAT5b (WT or Lysine-to-Arginine (KR) mutant) was cotransfected, followed by treatment with or without PRL for 30 min. Anti-Myc immunoprecipitates were blotted with anti-HA. (*F*) In PC3 cells, empty vector (EV), STAT5b WT, or STAT5b KR mutants were transfected along with pLHRE-luciferase reporter, followed by treatment with PRL for 6–12 h before luciferase activity assay. (*G*) Myc-STAT5b was transfected along with EV, PRLR WT, or PRLR K1–15R in 293T cells, followed by PRL treatment for 30 min. Anti-Myc immunoprecipitates were analyzed with indicated antibodies. (*H*) 293T cells were transiently transfected with PRLR and JAK2, followed by PRL treatment for 60 min. Immunoprecipitated JAK2 was analyzed for PRLR association or phospho-JAK2. (*I*) (*Left*) In 293T cells, PRLR WT and indicated PRLR mutants were transfected along with pLHRE-luciferase reporter, followed by PRL treatment for 6–12 h before luciferase activity assay. In 293T cells, EV, CBP, or SIRT2 was cotransfected with PRLR and luciferase reporter or siRNA of control (CTL), CBP, or SIRT was cotransfected with PRLR and luciferase reporter. (*Right*) Luciferase activity assay was performed under the same conditions as above.

tagged full-length PRLR along with the above Myc-tagged PRLR cytoplasmic loop truncates (Fig. S1*D*). The subsequent coimmunoprecipitation results in Fig. 3*D* revealed that the interaction between the full-length PRLR and these PRLR cytoplasmic loop truncates was overall dependent on PRL and NAM treatment, although the interaction between truncates such as the 259–566 region and full-length PRLR became less dependent on PRL and NAM treatment. The effect of the K→R mutation on the protein-protein interaction between the PRLR cytoplasmic loop and full-length PRLR was examined. However, individual K→R substitution of all 15 acetylated lysine sites exhibited no apparent defect in dimerization between the PRLR cytoplasmic loop and full-length PRLR (Fig. S3*C*). These results indicate that two PRLR protein molecules may interact with each other through multiple regions within their cytoplasmic loops during dimerization and may be modulated by acetylation on multiple sites.

To assess cytokine receptor dimerization in living cells, we used FRET to measure the energy transfer between monomeric YFP and monomeric CFP as a function of distance (8). We prepared two PRLR constructs with the CFP tag and YFP tag fused to the C-terminal end of PRLR (i.e., PRLR-CFP and PRLR-YFP, respectively). CHO cells were used for human PRLR FRET analysis because these cells do not respond to human PRL unless exogenous PRLR of human origin is transfected (9). Both CFP- and YFP-tagged PRLR was observed to localize on the cell membrane (Fig. 3*E*). Although a high FRET signal of WT PRLR

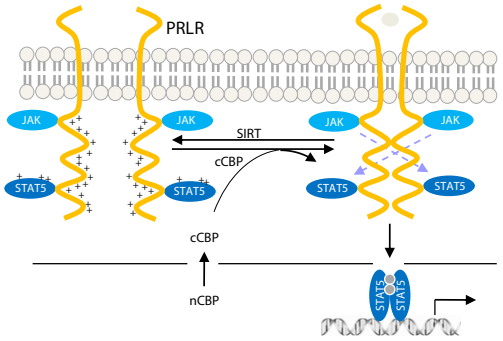

Fig. 5. Model of acetylation-dependent PRLR-STAT5 route activation. The cytoplasmic CBP (basal and CBP exported from nuclei on PRL treatment) is responsible for PRLR cytoplasmic loop acetylation on multiple sites. Acetylated PRLR undergoes dimerization between two monomers within their cytoplasmic loops, followed by STAT5 activation. CBP is also responsible for STAT5 acetylation-dependent dimerization and transcriptional activation. SIRT (SIRT2) can reverse this CBP-dependent PRLR-STAT5b route activation. cCBP, CBP in cytoplasm; nCBP, CBP in nucleus.

expressed as CFP and YFP forms in CHO cells was observed in the absence of PRL (Fig. 3 *E* and *F*), PRL stimulation routinely increased FRET signal intensity of WT PRLR by a factor of 2- to 3-fold (Fig. 3 *E* and *F*). Because individual K→R mutation had little effect on PRLR dimerization as revealed by coimmunoprecipitation analysis (Fig. S3*C*), we examined PRLR with multiple K→R mutations for FRET. Receptors with triple or multiple K→R mutations reduced FRET signal intensity but retained increased dimerization in response to PRL treatment (Fig. 3 *E* and *F*). When all 15 acetylatable lysine sites were substituted with arginine (K1–15R), however, FRET signal became undetectable (Fig. 3 *E* and *F*). PRLR (K1–15R) also showed reduced dimerization in coimmunoprecipitation experiments (Fig. 3*G*). In contrast, when all 15 lysine sites were replaced with alanine (K1–15A), PRLR became more sensitive in FRET signal induction and protein-protein interaction (Fig. 3 *E*–*G*). A basal level of receptor dimerization detected with different approaches here is in agreement with the fact that a basal level of PRLR-CBP association or a basal level of PRLR acetylation was visualized under the conditions used.

STAT5b Dimerization Relies on the Family-Conserved Acetylation Site Within the C-Terminal Region. STAT5 is the principal signaling factor recruited by the PRLR cytoplasmic loop for activation. To identify acetylation sites of STAT5, acetylated STAT5b proteins were immunopurified from 293T cells overexpressing CBP and analyzed with MS. Both MS and site-directed mutagenesis results revealed that K694 and K701 within the SH2-dimerization domain and K359 within the DNA-binding domain were major acetyl-lysine sites of STAT5b protein (Fig. 4 *A* and *B*). It is worth noting that K694 and K701 sites could be independently acetylated and that STAT5b phosphorylation on Y699 was not a prerequisite for acetylation of these two adjacent lysine sites, as reflected from the mass spectra. To confirm endogenous STAT5b acetylation induction, polyclonal antibodies were prepared for K359-, K694-, and K701-acetylated STAT5b (Fig. S1*E*). Using these specific antibodies, we clearly detected STAT5b acetylation induction on these three lysine sites by PRL in T47D cells, albeit with different patterns (Fig. 4*C*). STAT5b and PRLR acetylation share common features: (*i*) depletion of CBP with siRNA largely abolished STAT5b acetylation in response to PRL treatment in T47D cells (Fig. 4*D*); (*ii*) STAT5b was preferentially acetylated by CBP when compared with other HAT in 293T cells (Fig. S4*A*); and (*iii*) pretreatment of the cells with NAM and, to a lesser extent, TSA enhanced CBP-mediated STAT5b acetylation (Fig. S4*B*). K694 and K701 of STAT5b are located in close proximity to the interface of the STAT5b dimer (Fig. S4*C*) (10). To test whether acetylation affects STAT5b dimerization, we cotransfected Myc-tagged and HA-tagged STAT5b in STAT5-null PC3 cells for STAT5/STAT5 coimmunoprecipitation analysis. PC3 is a prostate cancer cell line with deletion mutations of three STAT (i.e., stat3, stat5a, stat5b) genes (11). STAT5b with K694R substitution or, to a lesser extent, K701R substitution impaired STAT5b dimerization, whereas STAT5b with K359R substitution showed a minimal but repeatable positive effect on STAT5b dimerization (Fig. 4*E* and Fig. S4*D*). We used PC3 to test STAT5b acetylation on transcription. STAT5b with K701R substitution showed a minor effect on STAT5b transcriptional activation, whereas STAT5b with K359R or K694R substitution or K694/K701R double mutation apparently attenuated STAT5b transcriptional activity, as assayed by luciferase induction driven by the Lactogenic Hormone Responsive Element (pLHRE) promoter (Fig. 4*F*). These results indicate that acetylation on multiple lysine sites within different domains coordinately regulates transcriptionally active STAT5b dimer formation.

In lieu of the significance of cytokine receptor dimerization for signal transduction, we examined STAT5b recruitment and activation by PRLR K1–15R. Although PRLR K1–15R mutant still associated with STAT5b, Y699 phosphorylation and K694 acetylation were abolished (Fig. 4*G*). Both WT PRLR and PRLR K1–15R mutant recruited JAK2 constitutively and responded to ligand stimulation for JAK2 autophosphorylation (Fig. 4*H*). These findings agreed with reports that cytokine receptor dimerization is needed for STAT activation but not for STAT or JAK docking (12–14). None of the single PRLR K→R mutants impaired STAT5b recruitment and STAT5b phosphorylation on Y699 (Fig. S4 *E* and *F*). The fact that both WT PRLR and PRLR K1–15R exhibited similar ligand-binding efficiency in FACS analysis (Fig. S4*G*) suggests that PRLR with multiple K→R substitution in its cytoplasmic loop did not alter its extracellular domain activity in ligand recruitment. When PRLR downstream STAT5-dependent reporter activity was analyzed, PRLR largely abolished transcriptional activation only when all acetylated lysines were replaced with arginines (i.e., K1–15R) (Fig. 4*I Left*). In contrast, PRLR K1–15A mutation showed an increased response to PRL in terms of STAT5-dependent reporter activation (Fig. 4*I Left*). PRLR-T539A mutant inhibited STAT5b activation, whereas PRLR-T539D mutant showed normal STAT5b activation (Fig. 4*I Left*), supporting the finding that CBP can associate with PRLR on phospho-T539, leading to both PRLR and STAT5b activation. The opposite effects of CBP and SIRT2 on PRLR in STAT5b-dependent transcriptional activation were obvious, as revealed either by overexpression of ectopic CBP or SIRT2 gene or by depletion of endogenous CBP or SIRT2 in 293T cells (Fig. 4*I Right*). These results clearly demonstrate that CBP-catalyzed acetylation plays a critical role from PRLR to its downstream STAT5b activation.

Discussion

Dimerization has evolved as a general mechanism to bestow cellular proteins with functions from signal transduction to transcriptional activation (15, 16). Here, we demonstrate that PRLR undergoes dynamic cytoplasmic loop dimerization that is independent of extracellular dimerization but tightly regulated by acetylation in cells; cytoplasmic loop-dimerized PRLR then activates STAT5b, which is also acetylated by CBP and undergoes acetylation-dependent homodimerization (Fig. 5). Among type I cytokine receptors, PRLR has a long cytoplasmic loop, which is lysine-rich (29 lysines vs. 5 arginines). Although a longer loop can recruit more signaling molecules for activation, it becomes more difficult to undergo homodimerization, presumably because it carries more positive-charged residues. Acetylation provides such a nuance modulation by neutralizing the positive charges along the loop, leading to close proximity within multiple regions. This is most likely a common mechanism shared among type I cytokine receptors because different type I cytokine receptors, including erythropoietin receptor (EPOR), have all been found to undergo acetylation-dependent homodimerization. For EGF receptor

(EGFR) dimer, the intrinsic kinase domains of the two monomers have to be brought close enough to phosphorylate each other (5). Although cytokine receptors recruit JAK and STAT constitutively (2), acetylation brings two receptor loops into close proximity, a step required for STAT activation, which is quite similar to EGFR dimer autophosphorylation.

The basal level of cytoplasmic CBP could be responsible for PRLR activation initiation, followed by continuous CBP supply from nuclei. CBP activation by cytokine treatment is a receptor dimerization-independent event (i.e., CBP nuclear export, CBP cytokine receptor association, CBP-mediated cytokine receptor acetylation). Although the mechanism responsible for CBP nuclear exportation on PRL treatment remains unclear, JAK tyrosine kinase activity is unlikely involved in CBP cytoplasmic accumulation, because JAK2 depletion showed no effect on this event. Although the bromodomain of CBP can provide a modular interaction with acetylated lysines (17), PRLR interacts with CBP within the N-terminal domain (amino acids 1–460), where NLS1 resides, and the C-terminal domain. Type I cytokine receptor acetylation by CBP appears to be indispensable for receptor activation and reflects dynamic conversion of the receptor cytoplasmic loop's proximity-independent signaling event into the dependent one. CBP propagates acetylation from the membrane-proximal region to the membrane-distal region. This indicates that CBP may either interact with PRLR within multiple regions or slide along the loop to acetylate multiple sites of the loop as well as STAT proteins recruited by the loop.

It becomes clearer now that different STAT members activated by cytokines can be acetylated by CBP/p300 on multiple sites within different domains. Surprisingly enough, the only conserved acetylation site among STAT members is that of the SH2-dimerization domain, which resides in front of the family-conserved phosphotyrosine site. Cytokine-activated STAT switches from transcriptionally inactive dimer via protein interaction within the β-barrel DNA-binding domain into transcriptionally active dimer via protein interaction within the C-terminal SH2 dimerization domain (18, 19). In cytokine-activated STAT1, STAT4, and STAT6, the C-terminal SH2 dimerization domain-conserved lysine is acetylated and plays a prominent role in their homodimerization. Lacking this lysine in front of Y705, STAT3 is preferentially acetylated on K685, which resides on the external surface of the SH2 domain to form hydrogen bonds with two phenylalanine residues of the hydrophobic core of the SH2 domain (20). Acetylation on K685 disrupts the hydrogen bonds, leading to a conformational change necessary for active STAT3 dimer formation (21).

Hedgehog-induced receptor cytoplasmic domain phosphorylation creates a local negatively charged environment and induces a conformational switch and dimerization in a seven-transmembrane receptor protein (22). Likewise, acetylation creates a local environment that is less positively charged for protein contact. Thus, acetylation and deacetylation may provide a more general rheostat-like function than serine phosphorylation does for transmembrane receptors, regardless of the loop length, to undergo dimerization and dedimerization during intracellular signal transduction.

Materials and Methods

Plasmids, Antibodies, and Cell Culture. Plasmids, antibodies, and cell culture are discussed in *SI Materials and Methods*.

MS Analysis of Acetylated Lysine Sites. PRLR or STAT5b proteins, immunoprecipitated from 293T cells transfected with PRLR or STAT5b along with CBP, were resolved by 10% (w/v) SDS/PAGE and visualized by Coomassie blue staining. The bands of PRLR and STAT5b (1–2 mg) were excised and subjected to MS analysis provided by the Taplin Biological Mass Spectrometry Facility at Harvard Medical School. MS analysis of other acetylated lysine sites is discussed in *SI Materials and Methods*.

Immunoprecipitation and Western Blot Analysis, Luciferase Reporter Analysis, siRNA Knockdown, in Vitro Acetylation Assay, and Flow Cytometry Analysis. These processes are discussed in *SI Materials and Methods*.

FRET Assay. Photobleaching FRET imaging was conducted with a Nikon Eclipse TE2000-U microscope using a 60× oil objective lens coupled to a CoolSNAP HQ CCD camera (Roper Scientific). All imaging filters were from Chroma. They were YFP (HQ500/20×, Q515LP, HQ535/30M), CFP (D436/20×, 455DCLP, D480/40M), and YFP Photobleach (D535/50×, dichroic full mirror, metal slug). The spectrally corrected FRET efficiency was calculated according to the published protocol (23).

ACKNOWLEDGMENTS. We thank T. Welte (University of Texas Medical Branch, Galveston, TX) for STAT5b cDNA construct, P. S. Rotwein for pLHRE-luciferase reporter construct, T. P. Yao (Duke University, Durham, NC) for HA-tagged and Myc-tagged mouse CBP cDNA constructs, D. M. Heery (University of Nottingham, UK) for CFP-mouse CBP cDNA construct, X. J. Yang (McGill University Health Center, Canada) for some GST-CBP domain constructs, and E. Seto (H. Lee Moffitt Cancer Center and Research Institute, Tampa, FL) for HDAC6 and HDAC3 cDNA constructs. We thank K. Heflin and X. L. Liu for technical assistance; and our colleagues A. Ayala, J. Marshall, R. Page, and J. S. Reichner for discussion and critical reading of this manuscript. This work was supported by funds from the National Institutes of Health (to Y.E.C.).

1. Ihle JN, Kerr IM (1995) Jaks and Stats in signaling by the cytokine receptor superfamily. *Trends Genet* 11:69–74.
2. Constantinescu SN, Huang LJ, Nam H, Lodish HF (2001) The erythropoietin receptor cytosolic juxtamembrane domain contains an essential, precisely oriented, hydrophobic motif. *Mol Cell* 7:377–385.
3. Muthukumaran G, Kotenko S, Donnelly R, Ihle JN, Pestka S (1997) Chimeric erythropoietin-interferon gamma receptors reveal differences in functional architecture of intracellular domains for signal transduction. *J Biol Chem* 272:4993–4999.
4. Gadd SL, Clevenger CV (2006) Ligand-independent dimerization of the human prolactin receptor isoforms: Functional implications. *Mol Endocrinol* 20:2734–2746.
5. Zhang X, Gureasko J, Shen K, Cole PA, Kuriyan J (2006) An allosteric mechanism for activation of the kinase domain of epidermal growth factor receptor. *Cell* 125:1137–1149.
6. Cohen HY, et al. (2004) Acetylation of the C terminus of Ku70 by CBP and PCAF controls Bax-mediated apoptosis. *Mol Cell* 13:627–638.
7. Tang XL, et al. (2007) Acetylation-dependent signal transduction for type I interferon receptor. *Cell* 131:93–105.
8. Biener E, et al. (2003) Ovine placental lactogen-induced heterodimerization of ovine growth hormone and prolactin receptors in living cells is demonstrated by fluorescence resonance energy transfer microscopy and leads to prolonged phosphorylation of signal transducer and activator of transcription (STAT)1 and STAT3. *Endocrinology* 144:3532–3540.
9. Perrot-Applanat M, Gualillo O, Buteau H, Edery M, Kelly PA (1997) Internalization of prolactin receptor and prolactin in transfected cells does not involve nuclear translocation. *J Cell Sci* 110:1123–1132.
10. Neculai D, et al. (2005) Structure of the unphosphorylated STAT5a dimer. *J Biol Chem* 280:40782–40787.
11. Clark J, et al. (2003) Genome-wide screening for complete genetic loss in prostate cancer by comparative hybridization onto cDNA microarrays. *Oncogene* 22: 1247–1252.
12. Klingmüller U, Bergelson S, Hsiao JG, Lodish HF (1996) Multiple tyrosine residues in the cytosolic domain of the erythropoietin receptor promote activation of STAT5. *Proc Natl Acad Sci USA* 93:8324–8328.
13. Behncken SN, et al. (2000) Growth hormone (GH)-independent dimerization of GH receptor by a leucine zipper results in constitutive activation. *J Biol Chem* 275: 17000–17007.
14. Lu X, Huang LJ, Lodish HF (2008) Dimerization by a cytokine receptor is necessary for constitutive activation of JAK2V617F. *J Biol Chem* 283:5258–5266.
15. Weiss A, Schlessinger J (1998) Switching signals on or off by receptor dimerization. *Cell* 94:277–280.
16. Amoutzias GD, Robertson DL, Van de Peer Y, Oliver SG (2008) Choose your partners: Dimerization in eukaryotic transcription factors. *Trends Biochem Sci* 33:220–229.
17. Dhalluin C, et al. (1999) Structure and ligand of a histone acetyltransferase bromodomain. *Nature* 399:491–496.
18. Mao X, et al. (2005) Structural bases of unphosphorylated STAT1 association and receptor binding. *Mol Cell* 17:761–771.
19. Mertens C, et al. (2006) Dephosphorylation of phosphotyrosine on STAT1 dimers requires extensive spatial reorientation of the monomers facilitated by the N-terminal domain. *Genes Dev* 20:3372–3381.
20. Becker S, Groner B, Müller CW (1998) Three-dimensional structure of the Stat3β homodimer bound to DNA. *Nature* 394:145–151.
21. Yuan ZL, Guan YJ, Chatterjee D, Chin YE (2005) Stat3 dimerization regulated by reversible acetylation of a single lysine residue. *Science* 307:269–273.
22. Zhao Y, Tong C, Jiang J (2007) Hedgehog regulates smoothened activity by inducing a conformational switch. *Nature* 450:252–258.
23. Miyawaki A, Tsien RY (2000) Monitoring protein conformations and interactions by fluorescence resonance energy transfer between mutants of green fluorescent protein. *Methods Enzymol* 327:472–500.